Graptolite community responses to global climate change and the Late Ordovician mass extinction

H. David Sheets[a,1], Charles E. Mitchell[b], Michael J. Melchin[c], Jason Loxton[d], Petr Štorch[e], Kristi L. Carlucci[b], and Andrew D. Hawkins[b]

[a]Department of Physics, Canisius College, Buffalo, NY 14208; [b]Department of Geology, University at Buffalo, The State University of New York, Buffalo, NY 14260; [c]Department of Earth Sciences, St. Francis Xavier University, Antigonish, NS, Canada B2G 2W5; [d]Department of Earth Sciences, Dalhousie University, Halifax, NS, Canada B3H 4R2; and [e]Institute of Geology, The Czech Academy of Sciences, 165 00 Prague 6, Czech Republic

Edited by Michael Foote, University of Chicago, Chicago, IL, and accepted by Editorial Board Member David Jablonski May 20, 2016 (received for review February 6, 2016)

Mass extinctions disrupt ecological communities. Although climate changes produce stress in ecological communities, few paleobiological studies have systematically addressed the impact of global climate changes on the fine details of community structure with a view to understanding how changes in community structure presage, or even cause, biodiversity decline during mass extinctions. Based on a novel Bayesian approach to biotope assessment, we present a study of changes in species abundance distribution patterns of macroplanktonic graptolite faunas (~447–444 Ma) leading into the Late Ordovician mass extinction. Communities at two contrasting sites exhibit significant decreases in complexity and evenness as a consequence of the preferential decline in abundance of dysaerobic zone specialist species. The observed changes in community complexity and evenness commenced well before the dramatic population depletions that mark the tipping point of the extinction event. Initially, community changes tracked changes in the oceanic water masses, but these relations broke down during the onset of mass extinction. Environmental isotope and biomarker data suggest that sea surface temperature and nutrient cycling in the paleotropical oceans changed sharply during the latest Katian time, with consequent changes in the extent of the oxygen minimum zone and phytoplankton community composition. Although many impacted species persisted in ephemeral populations, increased extinction risk selectively depleted the diversity of paleotropical graptolite species during the latest Katian and early Hirnantian. The effects of long-term climate change on habitats can thus degrade populations in ways that cascade through communities, with effects that culminate in mass extinction.

abundance | climate change | extinction | macroevolution | selection

Mass extinctions affect communities over a range of hierarchical levels of organization (1, 2). Droser et al. (1) described four levels of community impacts, ranging from the broad scale of the development or loss of entire ecosystems to the fine scale of abundance changes within a single community. Studies of community changes among fossil marine invertebrates based on the occurrence of genera or broad functional groups have yielded interesting insights about the nature of mass extinctions, particularly the apparent decoupling of taxonomic and ecological impacts of mass extinction (e.g., refs. 1 and 2). Discussions of the ecological impact of mass extinction typically focus on the idea that communities are disrupted by the loss of species diversity (3, 4), or keystone species (5). Few studies (e.g., refs. 6 and 7) have examined within-community changes using abundance data collected from fossil invertebrate communities, but those few have produced novel and unexpected insights. In their analyses of terrestrial plant communities, where species (or generic) abundance data are the norm, McElwain et al. (8) demonstrated that fine-scale community changes may occur before mass extinctions as well as in the wake of those events, and that relative abundance curves revealed changes in community structure over the time span of a mass extinction event. Similarly, recent work on the response of modern biotas to anthropogenic effects on habitats and species distributions indicates that striking changes in the species abundance structure of communities may precede, and possibly presage, species losses (9, 10).

We consider here the fine-scale impact of climate change on planktonic communities during the Late Ordovician mass extinction (LOME) and the immediately preceding interval (~447–444 Ma). The loss of graptolite biodiversity in the LOME, accompanied by the wholesale extinction of the previously dominant Diplograptina (taxonomic use follows ref. 11) and their replacement by the previously marginal, high-latitude Neograptina (12–16), provides an opportunity to study the impact of climate change on a macroplanktonic invertebrate fauna over several million years during an interval of unusual species turnover (17, 18). A focus on climate change over geological timescales as a driver of extinction dynamics leads us to ask whether there is evidence of ecological community changes in the interval leading up to mass extinction. Do ecological communities collapse as species go extinct, or do environmental conditions cause disruptions of community structures that result in species extinctions, or do both species and communities react in similar ways to environmental insults? Examination of marine planktonic community structures before the main pulse of a mass extinction may yield insights about both the dynamics of the extinction process and the impact of community structure on changes on biodiversity—insights that may be of use in our efforts to understand the current accelerated rates of community change and species loss.

Planktic graptolite species may be grouped into two major ecological groups based on their habitat affinities, corresponding patterns of resource utilization, and species turnover dynamics

Significance

Climate change during Late Ordovician mass extinction drove an ecologically selective decline in the abundance of deep-water macrozooplankton, accompanied by a shift to simpler, less even communities. These results indicate that the species abundance structure of planktic communities may be a leading indicator of the effects of climate change on biodiversity and a more sensitive gauge of those effects than taxonomic diversity change alone. Additionally, we present a Bayesian likelihood method of habitat inference that may be applicable to other similar cases.

Author contributions: H.D.S., C.E.M., M.J.M., and A.D.H. designed research; H.D.S., C.E.M., M.J.M., J.L., P.S., K.L.C., and A.D.H. performed research; H.D.S., C.E.M., and J.L. analyzed data; and H.D.S., C.E.M., and M.J.M. wrote the paper.

The authors declare no conflict of interest.

This article is a PNAS Direct Submission. M.F. is a guest editor invited by the Editorial Board.

See Commentary on page 8349.

[1]To whom correspondence should be addressed. Email: sheets@canisius.edu.

This article contains supporting information online at www.pnas.org/lookup/suppl/doi:10.1073/pnas.1602102113/-/DCSupplemental.

(19, 20). One group is thought to have inhabited a deep-water biotope within the twilight or mesopelagic zone below the surface mixed layer (Fig. S1), with their peak diversity and abundance associated with productivity driven by nutrient upwelling at the edges of continental shelves from the oxygen minimum zone of a highly stratified ocean. The majority of graptolite species, however, appear to have occupied the relatively sunlit, surface mixed layer (epipelagic zone) of the ocean. The mesopelagic zone today is commonly separated from the overlying surface mixed zone by the pycnocline. This hydrographical boundary may have contributed to the segregation of pelagic graptolites within two more-or-less discrete habitats: the mesopelagic and epipelagic biotopes. After death, all these graptolites settled to form mixed assemblages on the sea floor, with epipelagic graptolites present at relatively onshore as well as at more offshore localities, whereas mesopelagic species occur only in strata deposited near the shelf margin and beyond. Changes in deep-ocean circulation and oxygenation driven by climate change contributed to the Ordovician mass extinction (12, 13, 15, 21, 22), which suggests that the mesopelagic biotope may have been the most vulnerable and should exhibit disproportional extinction.

The LOME is associated with a shift from the greenhouse climate that had dominated most of the Cambrian to Mid-Ordovician metazoan macroevolutionary radiations to icehouse conditions through an interval of increasingly cool and unstable conditions during the Late Ordovician (23–25). Hirnantian (latest Ordovician) glaciation lowered sea levels by some 70–100 m (26, 27), reduced tropical sea surface temperatures by ∼6 °C (22, 26), and increased oxygenation of the deep oceans (22, 28, 29). In combination, these changes appear to have reduced the supply of nutrient-rich, denitrified waters, which led to changes in the composition of the phytoplankton community at most sites formerly occupied by the diverse shelf-edge graptolite communities (21, 22, 30).

In this study, we ask whether the ecological composition and structure of graptolite communities exhibited changes during the interval of climate deterioration and gradual species losses that preceded the onset of major Hirnantian glaciation, and presaged the dramatic taxonomic turnover that accompanied that event. Further, we ask whether those changes in community abundance structure provide novel insights into the mass extinction that differ from those suggested by the well-documented history of changes in the species composition of Late Ordovician faunas (17).

We address these questions by analysis of species abundance patterns through measured stratigraphic sections at two localities from the northwestern passive margin of Laurentia (Fig. S2 and Datasets S1 and S2). The Vinini Creek site (Nevada; hereafter VC) records deposition in a bathyal continental slope to ocean floor setting, slightly south of the paleoequator (15, 31). The Blackstone River site (Ogilvie Mountains, Yukon, Canada; hereafter BR) was a shallower site located ∼3,000 km away, on the continental shelf, north of the paleoequator (32, 33). Additionally, paleoenvironmental proxy data are available at these sites (21, 22, 30, 34) that permit independent characterization of paleoceanographic changes. These data include ε_{Nd} values (Fig. 1), from which we reconstruct relative sea level changes at BR and VC (see ref. 34 and *SI Text* for further discussion) that we denoted as cycles O4a to O6b, following refs. 35 and 36.

Results

With the aid of a Bayesian biotope assignment procedure with a 90% confidence level cutoff, we identified 12 late Katian diplograptine species at BR and VC as mesopelagic (Fig. 1) and 9 species as epipelagic (Dataset S3). The remaining 22 diplograptine species had indeterminate biotope affinities. These results were consistent with a detrended correspondence analysis (DCA) based depth assignment of the same species and localities (Dataset S3 and Fig. S3). Neograptine species invade the paleotropics immediately before the start of the Hirnantian Age (14), and, thus, only four of these species occur within the latest Katian at the study sites (Dataset S2); two emerge as epipelagic, but the other two are too rare to classify.

The species compositions of the late Katian graptolite faunas at the BR and VC sites are very similar. At both sites, a small subset of species are regularly among the most abundant; however, the particular species that dominate each collection varies substantially among successive collections. Furthermore, although nearly all of the species present at BR are also present at VC, the dominance structure of communities differs substantially between the two sites. Epipelagic species are significantly more abundant than mesopelagic species (higher total specimen counts; Table S1 and Fig. 1*A*) at BR and are more frequently among the most abundant species in nearly all BR samples, whereas, at VC, it is the mesopelagic species that have the highest total specimen counts. These differences in biotope dominance match expectations from the depositional setting of the two sites. Geological context, lithofacies, and associated fauna (19, 20, 28, 29) suggest that BR represents a midshelf site, whereas the VC site was on the continental slope to ocean floor. Because the species occurrences at BR were not used in the Bayesian biotope inference process, this result serves as a cross-validation of the biotope assignments themselves. We also examined species dominance patterns at five coeval sites in South China, which also were not used as part of the biotope inference process, and they too exhibit faunal contrasts that match expectations from their geological setting (Figs. S4 and S5).

The community structure statistics for VC and BR (Fig. 1) exhibit peak values of Shannon information (H) and evenness (E) in the *Dicellograptus ornatus* to mid-*Paraorthograptus pacificus* zones (see also Datasets S4 and S5), during the interval of the O4 relative water depth cycle (34). The highest recorded H and E values occur in the early *P. pacificus* Zone interval (O4b) when abundant black shales were deposited beneath a strongly developed denitrification zone at the site (21, 22). Biomarkers (Fig. 1*B*) indicate the presence of a predominantly cyanobacterial phytoplankton community in this interval (30). Graptolite communities at this oceanic site exhibit generally lower H and E during times of lower relative water depth (Fig. 1; see also Figs. S6–S8). Evenness values at both sites are significantly lower during the *Diceratograptus mirus* interval (mean 0.293 at VC, 0.338 at BR), before the first Hirnantian glacial advance, compared with pre-*mirus* values (pre-*mirus* mean 0.4372 at VC, 0.54556 at BR, one-tailed t-Test, df = 9; $t = 2.11$; $P = 0.032$ at VC and df = 13, $t = 3.15$, $P = 0.004$ at BR). The Aikake Information Criteria based model choice procedure used to determine the species abundance distribution (SAD) model that best describes the graptolite abundance data for each sample (Dataset S6) produced clear assignments to either a simple or a complex community structure for all but one of the sampled VC assemblages. Complex community structures are absent from VC within the *D. mirus* Subzone. Community structure and evenness reach their lowest levels coincident with the major faunal turnover at the beginning of the Hirnantian Age (base of the *Metabolograptus extraordinarius* Zone) during the O5a maximum flooding interval.

Graptolite communities at the study sites also exhibit a significant change in biotope structure over the course of the late Katian. Faunas at both sites exhibit small fluctuations in the proportion of epipelagic and mesopelagic species through the late Katian O4 interval (Fig. 1; 100–54% mesopelagic at VC and 70–44% at BR), roughly in step with relative water depth changes and changes in H and E. Contingency tests (vassarstats.net/) for changing proportions based on specimen counts reveal sharp and highly significant declines in the dominance of mesopelagic species (from 35% to 11%; Table S2) and the abundance of mesopelagic specimens over the course of the pre-*D. mirus* interval at the BR site (from 51.6% to 4.7% mesopelagic; Table S3).

The differences in pattern of changing composition between these two sites partly reflects their different ecological settings

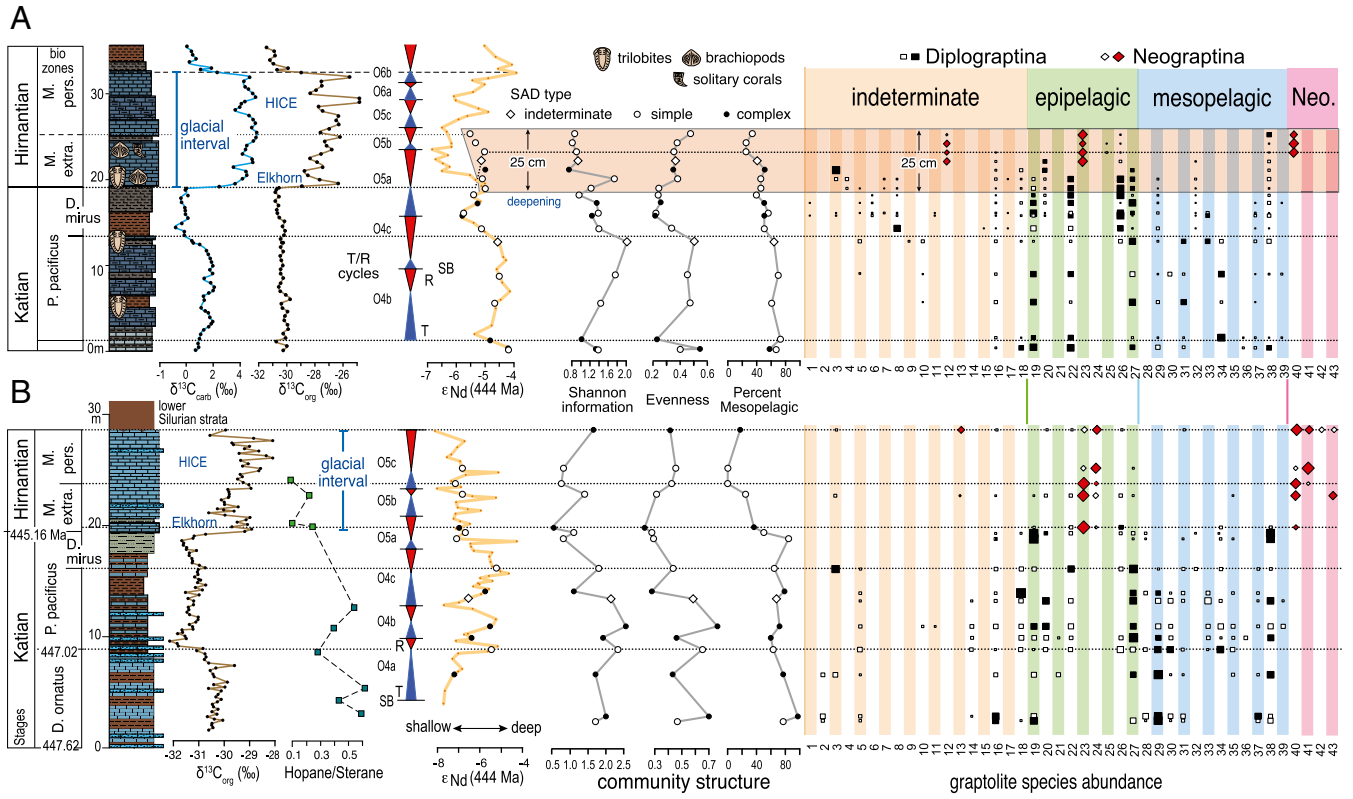

Fig. 1. Species biotope assignments, abundances and community structure obtained from bulk sampled Late Ordovician graptolite faunas plotted against schematic representations of the stratigraphic successions (21, 34, 41) and geochemical proxies for environmental change at (*A*) BR (note expanded vertical scale in shaded interval at this site) and (*B*) VC. Carbon isotope values ($\delta^{13}C_{organic}$ and $\delta^{13}C_{carbonate}$) (21) and hopane/sterane biomarker ratios (30) document the timing of faunal change relative to changes in phytoplankton communities and the basal Hirnantian Elkhorn and the mid-Hirnantian (HICE) carbon isotopic excursions (22). T/R cycles are relative sea level change: transgressions and regressions, respectively, separated by inferred sequence boundaries (SB) based on ε_{Nd} values and interpretation in ref. 34. Values for ε_{Nd} at graptolite sample levels are based on piece-wise linear interpolation between flanking measured values. Symbols for Shannon information, evenness, percent of mesopelagic species, and interpolated ε_{Nd} values correspond to the SAD type for each sample (key at top of figure). Species abundance data and key to numbering are presented in Datasets S4 and S5. Species are grouped according to inferred biofacies affiliation and clade membership; sizes of symbols for species occurrences are proportional to the log of the number of attributed specimens in each collection. See ref. 34 for explanation of lithological symbols.

relative to the graptolite habitats. As the evenness (E) and diversity (H) declined through the latest Katian, the preglacial communities at the midshelf BR site became ever more strongly dominated by a smaller number of epipelagic species as the oceanic water mass moved offshore [indicated by the upsection shallowing recorded in Neodymium isotope ratio (ε_{Nd}) values] (34). In contrast, specimen counts from the bathyal VC site reveal a more subdued shift toward faunas, with an increased proportion of specimens attributed to epipelagic species (Table S3). Those shelf-edge communities maintained their more dominantly mesopelagic species composition (60–80%) until nearly the end of the Katian, even as E and H declined through the *D. mirus* interval. Local depositional conditions also affected the record of faunal response. In particular, the O5a transgressive interval is thicker and more completely sampled at BR (Fig. 1), whereas this interval is strongly condensed at VC (34). At both sites, however, the available data from the O5a transgressive interval indicate that faunas failed to recover as they did in the preceding transgressive to highstand intervals: H, E, and proportion of mesopelagic species remain like those reached during the relative sea level fall and reach their lowest levels coincident with the O5a minimum in ε_{Nd} values. The correspondence between ε_{Nd} values and community diversity measures (H, E, and proportion of mesopelagic species) in samples from O5 succession are markedly different from those of the preceding O4 samples (Fig. 1 and Fig. S8). These relationships indicate that the graptolite faunas tracked shifting water masses during the Late Ordovician relative sea level changes (as recorded in the changing ε_{Nd} values) and that these relationships altered significantly during the course of the latest Katian environmental change.

The late Katian O4b–c interval within the *P. pacificus* Zone corresponds globally to an interval of relatively warm sea surface temperatures (24) and climate amelioration that is often referred to as the Boda Event (37–39). Deposition of black shales, especially in regions of oceanic upwelling, was widespread (22), and global graptolite species diversity reached a Late Ordovician peak at this time (25, 40). As sea surface temperatures subsequently declined into the Hirnantian glaciation, extinction rates also rose and graptolite species diversity declined (13, 17). At the present study sites, most graptolite communities of the early *P. pacificus* interval are best fit by complex SAD models (Datasets S4 and S5). Samples from the subsequent *D. mirus* interval at VC exhibit lower evenness, and complex SAD models no longer match the observed patterns. Values of H decline toward the end of the *D. mirus* interval, and individuals of the remaining mesopelagic and epipelagic species become codominant. All of these signals appear to indicate that the community structure at VC became simpler, largely due to the decline in species diversity and concomitant preferential loss of deep-water taxa, so that there was less vertical niche subdivision during this interval at this site. Community changes at BR were more limited but again result in smaller communities dominated by a few epipelagic species joined by the invading Neograptina. Thus,

the basic character of each site (a predominantly mesopelagic, oceanic community at VC and a predominantly epipelagic mixed shelf community at BR) persisted, but the fine structure of community composition became increasingly different during the latest Katian, preglacial interval (Fig. 1). This contrast raises the possibility that ocean conditions above the abyssal VC site responded differently to Late Ordovician climate change than did the shelf seas above the BR site.

The onset of the glaciation early in *M. extraordinarius* Zone time is marked at both VC and BR by a decrease in ε_{Nd}, suggesting relative sea level fall, a strong positive excursion in $\delta^{13}C$, and the abrupt replacement of the diplograptine fauna by neograptine species. At both sites, the replacement of Diplograptina by Neograptina occurs during the early phase of relative sea level fall. After being absent from the paleotropics throughout the late Katian (14), the Neograptina invaded at the onset of the glacial epoch and immediately became the dominant species: Neograptines comprise 90–99% of specimens recovered in this interval at both sites, despite their different depositional settings. At VC, the appearance of the neograptine community is associated with hopane–sterane ratios that suggest the phytoplankton community shifted from cyanobacteria in O4 to dominantly green algae in O5. Concomitantly, observed $\delta^{14}N$ values suggest reduced denitrification in the local water column (21, 22, 30). During the Hirnantian at the bathyal VC site, 10 diplograptine species reappeared briefly in association with intervals of relative sea level rise, but diplograptines remained minor elements (0–8% of specimens) within communities dominated by Neograptina (Fig. 1; see also ref. 41). This pattern suggests that ecological stress on graptolite communities arising from changes in productivity patterns and displacement by the invading Neograptina exceeded a critical tipping point that led to the widespread collapse of the previous diplograptine community structure. The diplograptine species that persisted through the glacial interval as minor constituents of the reorganized neograptine communities were essentially "dead clades walking" (42). All of them went extinct during the postglacial extinction pulse (12, 13).

Conclusions

The picture that emerges of graptolite community structure from these two sites in the interval leading up to the mass extinction is of planktonic communities under stress due to the deteriorating conditions for mesopelagic taxa. Although sea level actually rose near the end of the interval leading up to the glaciation and the mass extinction interval, the oxygen minimum zone contracted and the supply of nutrients from denitrified deep ocean water decreased as a consequence of changes in deep-water ocean circulation patterns. These changes (and probably others, most notably lower sea surface temperature and increased seasonality) stressed graptolite communities, leading to reduced community complexity and evenness at both oceanic and midshelf sites. The species that most strongly declined, in terms of their individual contributions to community composition, were preferentially those adapted to the mesopelagic habitat. Brachiopod species reveal a similar selectivity (18). Extinction of the majority of the graptolite species making up these stressed communities did not occur, however, until the onset of the glacial interval (or even later), when diplograptines were replaced by the neograptine species that migrated into the paleotropics and diversified during the Hirnantian Age. This pattern of selectivity may have contributed to the unusually high losses of old, well-established graptolite species (positive age-dependent risk of extinction) during the LOME (17).

The dominantly epipelagic community at BR was consistently less complex and had lower evenness than VC communities, which were relatively even and complex with large mesopelagic components before the *D. mirus* Subzone interval. The graptolite communities at both study sites experienced significant change during the latest Katian Age, but the different responses at each site led to a divergence in community composition and abundances structures. Furthermore, relative sea level rise during the latest *D. mirus* interval did not restore the previous community structures. These features indicate that the observed changes in graptolite community structure were not a sampling artifact caused by shifting facies and eustatic sea level fall (43) and reinforce suggestions that carefully controlled analysis across multiple depositional environments is essential to understand the common cause effects of sea level and environmental changes on mass extinction (43, 44).

Graptolite community structure reveals evidence of environmentally induced stress on these organisms before the main pulse of mass extinction during the early Hirnantian. The changes in late Katian graptolite communities reflect the combined effects of species losses due to extinction and ecological reorganization driven by the effects of climate change on the distribution of nutrients, water column oxygenation, and phytoplankton community composition. Even the apparently abrupt change in communities at the start of the Hirnantian was predominantly a consequence of dramatic changes in community structure as opposed to imminent species extinctions, because many of these extinctions occurred hundreds of thousands of years after this ecological turnover event and neograptine invasion. Ecological stresses on communities, therefore, may not be obvious from species diversity patterns alone. Closer examination of community structures, habitat preferences, and abundance patterns provides unique information about the impacts of climate change before the onset of elevated rates of extinction.

Materials and Methods

Data Collection. We gathered species abundance data from bulk samples at the well-studied, deep-water Vinini Formation in central Nevada. All identifiable specimens of each species were counted, resulting in collection sizes from 166 to 606 identified specimens per horizon (Dataset S3). Bulk samples at the BR site in the Ogilvie Mountains of Yukon (Canada) were larger than at VC, and ranged from 124 to 3,072 identified specimens per sample. We preferentially sampled well-laminated, fine-grained sediments throughout both sections, seeking, as much as possible, to hold preservational and facies-related variance in assemblage composition to a minimum. Variation in ε_{Nd} values through the sections indicates that most samples represent the deeper parts of the series of relative water depth cycles present through the studied interval, adding to their taphonomic consistency.

Statistical Approaches: Determining the Biotope Affinity of Species. We used statistical procedures to estimate the biotope affinity (mesopelagic or epipelagic) of each of the species of Diplograptina present within late Katian strata at VC and BR. In addition to the species abundance data available for VC, we also used horizon-by-horizon records of species presence/absence from the *P. pacificus* Zone at 18 other localities to provide a strong contrast between deep-water and shallow water localities (Fig. S2 and Dataset S1). The Trail Creek, Idaho, and Dob's Linn, southern Scotland, sites provide additional data from deep oceanic settings, whereas sites at Truro Island, Eleanor Lake, and Cape Manning in the Canadian Arctic provide species occurrences from relatively shallow, midshelf to platform margin settings (ref. 22 and Dataset S1). A set of five sections in the Omulev Mountains of Siberia and six sections in the Chu-Ili Range of Kazakhstan expand the sample set beyond Laurentia and encompass a range of site conditions from deep back-arc to midshelf (Dataset S1). We used data from a set of five sections from South China to cross-validate the biotope assignments (*SI Text*).

We inferred biotope affinity through a novel Bayesian approach. We treated each collection horizon as an individual case, so that there were 20 shallow collections, 37 deep collections, 25 intermediate collections, and, excluding taxa seen in only one section, a total of 43 species in the analysis. The basic approach is to build a maximum likelihood model of finding each species at a shallow or deep horizon, given the observed patterns of presence and absence at each horizon at each locality and the biotope affinity of each species (see *SI Text* for analytical details). A Markov chain Monte Carlo (MCMC) search process was used to determine the posterior probability distribution of biotope affinity, starting from a prior probability of 0.5 for the biotope affinities of each species. This statistical modeling procedure assigns species with strong evidence of restriction to deep water a posterior probability of being mesopelagic that is close to 1, whereas those that appear regularly in shallow water sites will have probabilities of being

mesopelagic that are close to 0 (and vice versa). Intermediate values indicate contradictory or limited evidence. We categorized as mesopelagic those species that received a Bayesian posterior probability of being mesopelagic of >90%, and classed as epipelagic those with a mesopelagic probability of <10%; all others are indeterminate (Dataset S2). We chose a 10% confidence level because of the limited sample sizes. Twenty-three of the 40 Katian species present at VC and BR were confidently classified with this protocol (9 epipelagic and 14 mesopelagic) with the other 17 left in the indeterminate category (Datasets S3 and S4). In light of the very clear segregation of our sites and taxa into binary categories (shallow/epipelagic and deep/mesopelagic), we used DCA (45) to analyze the same set of data that we used in the Bayesian analysis as a means to assess the plausibility of the outcome of this new procedure.

Characterizing Community Structure. We described community structure via the Shannon information [$H = -\Sigma f_i \times \ln(f_i)$] and an E derived from H ($E = e^H/N$, where N is the number of species) to characterize the communities (see also Fig. S6 for a set of related rarefaction curves).

Additionally, we fit a series of SAD models (geometric, log series, and lognormal) to the data. The lognormal model differs from the geometric and log-series models in the number of species of intermediate abundances, and may be indicative of relatively complex communities with substantial species interactions and species interdependence (6). The geometric and log-series models have been interpreted as indicating relatively simple community structure, without extensive interaction among the species within the community. AIC model ranking (46) was used to determine which of the fit models should be considered as viable at each horizon (Dataset S6). We considered horizons to have a complex distribution if the weight of the lognormal model was above 90% and to have simple distribution if the combined weight of the simple distributions (geometric and log series) was above 90%. All other horizons are indeterminate.

ACKNOWLEDGMENTS. H.D.S., C.E.M., and M.J.M. conducted this research with financial support from the US National Science Foundation, Grant Division of Earth Sciences (EAR) 0418790. M.J.M. received financial support for this research through a Natural Sciences and Engineering Research Council of Canada (NSERC) Discovery Grant. P.Š. received support for work related to this project from the Grant Agency of the Czech Academy of Sciences (AS CR) through Grant IAA301110908. Finally, this paper is a contribution to The International Geosciences Programme (IGCP) 591—The Early to Middle Paleozoic Revolution.

1. Droser ML, Bottjer DJ, Sheehan PM, McGhee GR (2000) Decoupling of taxonomic and ecologic severity of Phanerozoic marine mass extinctions. *Geology* 28(8):675–678.
2. McGhee GR, Jr, Clapham ME, Sheehan PM, Bottjer DJ, Droser ML (2013) A new ecological-severity ranking of major Phanerozoic biodiversity crises. *Palaeogeogr Palaeoclimatol Palaeoecol* 370:260–270.
3. Brenchley PJ, Marshall JD, Underwood CJ (2001) Do all mass extinctions represent an ecological crisis? Evidence from the Late Ordovician. *Geol J* 36(3-4):329–340.
4. Hull PM, Darroch SAF (2013) Mass extinctions and the structure and function of ecosytems. *Ecosystem Paleobiology and Geobiology, The Paleontological Society Short Course, October 26, 2013*, Paleontological Society Papers, eds Bush AM, Pruss SB, Payne JL (Paleontol Soc, Boulder, CO), Vol 19, pp 1–42.
5. Solé RV, Saldaña J, Montoya JM, Erwin DH (2010) Simple model of recovery dynamics after mass extinction. *J Theor Biol* 267(2):193–200.
6. Wagner PJ, Kosnik MA, Lidgard S (2006) Abundance distributions imply elevated complexity of post-Paleozoic marine ecosystems. *Science* 314(5803):1289–1292.
7. Clémence M-E, Hart MB (2013) Proliferation of Oberhauserellidae during the recovery following the Late Triassic extinction: Paleoecological implications. *J Paleontol* 87(6): 1004–1015.
8. McElwain JC, Wagner PJ, Hesselbo SP (2009) Fossil plant relative abundances indicate sudden loss of Late Triassic biodiversity in East Greenland. *Science* 324(5934): 1554–1556.
9. Pandolfi JM, Lovelock CE (2014) Ecology. Novelty trumps loss in global biodiversity. *Science* 344(6181):266–267.
10. Dornelas M, et al. (2014) Assemblage time series reveal biodiversity change but not systematic loss. *Science* 344(6181):296–299.
11. Melchin MJ, Mitchell CE, Naczk-Cameron A, Fan JX, Loxton J (2011) Phylogeny and adaptive radiation of the Neograptina (Graptoloida) during the Hirnantian mass extinction and Silurian recovery. *Proc Yorks Geol Soc* 58(4):281–309.
12. Melchin MJ, Mitchell CE (1991) Late Ordovician extinction in the Graptoloidea. *Advances in Ordovician Geology*, Geological Survey of Canada Papers, eds Barnes CR, Williams SH, (Geol Surv Canada, Ottawa), Vol 90-9, pp 143–156.
13. Xu C, Melchin MJ, Sheets HD, Mitchell CE, Fan J (2005) Patterns and processes of latest Ordovician graptolite mass extinction and recovery based on data from South China. *J Paleontol* 79(5):842–861.
14. Goldman D, et al. (2011) Biogeography and mass extinction: Extirpation and reinvasion of Normalograptus species (Graptolithina) in the Late Ordovician palaeotropics. *Proc Yorks Geol Soc* 58(4):227–246.
15. Finney SC, Berry WBN, Cooper JD (2007) The influence of denitrifying seawater on graptolite extinction and diversification during the Hirnantian (Latest Ordovician) mass extinction event. *Lethaia* 40(3):281–291.
16. Bapst DW, Bullock PC, Melchin MJ, Sheets HD, Mitchell CE (2012) Graptoloid diversity and disparity became decoupled during the Ordovician mass extinction. *Proc Natl Acad Sci USA* 109(9):3428–3433.
17. Crampton JS, Cooper RA, Sadler PM, Foote M (2016) Greenhouse–icehouse transition in the Late Ordovician marks a step change in extinction regime in the marine plankton. *Proc Natl Acad Sci USA* 113(6):1498–1503.
18. Finnegan S, Rasmussen CM, Harper DA (April 27, 2016) Biogeographic and bathymetric determinants of brachiopod extinction and survival during the late Ordovician mass extinction. *Proc R Soc B*, 10.1098/rspb.2016.0007.
19. Cooper RA, Rigby S, Loydell DK, Bates DEB (2012) Palaeoecology of the Graptoloidea. *Earth Sci Rev* 112(1-2):23–41.
20. Cooper RA, Sadler P (2010) Facies preference predicts extinction risk in Ordovician graptolites. *Paleobiology* 32(2):167–187.
21. LaPorte DF, et al. (2009) Local and global perspectives on carbon and nitrogen cycling during the Hirnantian glaciation. *Palaeogeogr Palaeoclimatol Palaeoecol* 276(1-4): 182–195.
22. Melchin MJ, Mitchell CE, Holmden C, Štorch P (2013) Environmental changes in the Late Ordovician–Early Silurian: Review and new insights from black shales and nitrogen isotopes. *Geol Soc Am Bull* 125(11/12):1635–1670.
23. Trotter JA, Williams IS, Barnes CR, Lécuyer C, Nicoll RS (2008) Did cooling oceans trigger Ordovician biodiversification? Evidence from conodont thermometry. *Science* 321(5888):550–554.
24. Finnegan S, et al. (2011) The magnitude and duration of Late Ordovician–Early Silurian glaciation. *Science* 331(6019):903–906.
25. Cooper RA, Sadler PM, Munnecke A, Crampton JS (2014) Graptoloid evolutionary rates track Ordovician–Silurian global climate change. *Geol Mag* 151(2):349–364.
26. Brenchley PJ, et al. (1994) Bathymetric and isotopic evidence for a short-lived Late Ordovician glaciation in a greenhouse period. *Geology* 22(4):295–298.
27. Brenchley PJ (2004) End Ordovician glaciation. *The Great Ordovician Biodiversification Event*, eds Webby BD, Paris F, Droser ML, Percival IG (Columbia Univ Press, New York), pp 81–83.
28. Jones DS, Fike DA (2013) Dynamic sulfur and carbon cycling through the end-Ordovician extinction revealed by paired sulfate–pyrite δ34S. *Earth Planet Sci Lett* 363:144–155.
29. Zhou L, et al. (2015) Changes in marine productivity and redox conditions during the Late Ordovician Hirnantian glaciation. *Palaeogeogr Palaeoclimatol Palaeoecol* 420: 223–234.
30. Rohrssen M, Love GD, Fischer W, Finnegan S, Fike DA (2013) Lipid biomarkers record fundamental changes in the microbial community structure of tropical seas during the Late Ordovician Hirnantian glaciation. *Geology* 41(2):127–130.
31. Finney SC, Perry BD (1991) Depositional setting and palaeogeography of Ordovician Vinini Formation, central Nevada. Paleozoic Paleogeography of the Western United States 2: Pacific Section, eds Cooper JD, Stevens CH (Soc Sed Geol, Pacific Sect, Los Angeles), Vol 2, pp 747–766.
32. Lenz AC, McCracken AD (1982) The Ordovician–Silurian boundary, northern Canadian Cordillera: Graptolite and conodont correlation. *Can J Earth Sci* 19(6):1308–1322.
33. Loxton J, Melchin MJ, Mitchell CE, Senior SJH (2011) Ontogeny and astogeny of the graptolite genus *Appendispinograptus* (Li and Li, 1985). *Proc Yorks Geol Soc* 58(4): 253–260.
34. Holmden C, et al. (2013) Nd isotope records of late Ordovician sea-level change—Implications for glaciation frequency and global stratigraphic correlation. *Palaeogeogr Palaeoclimatol Palaeoecol* 386(18):131–144.
35. Harris MT, Sheehan PM (1997) Carbonate sequences and fossil communities from the Upper Ordovician–Lower Silurian of the Eastern Great Basin. *Brigham Young Univ Geol Stud* 42(1):105–128.
36. Jones DS, Creel RC, Rios BA (January 26, 2016) Carbon isotope stratigraphy and correlation of depositional sequences in the Upper Ordovician Ely Springs Dolostone, eastern Great Basin, USA. *Palaeogeogr Palaeoclimatol Palaeoecol*, 10.1016/j/palaeo.2016.01.036.
37. Fortey RA, Cocks LRM (2005) Late Ordovician global warming—The Boda event. *Geology* 33(5):405–408.
38. Armstrong HA, Baldini J, Challands TJ, Gröcke DR, Owen AW (2009) Response of the Inter-tropical Convergence Zone to Southern Hemisphere cooling during Upper Ordovician glaciation. *Palaeogeogr Palaeoclimatol Palaeoecol* 284(3-4):227–236.
39. Jiménez-Sánchez A, Villas E (2010) The bryozoan dispersion into the Mediterranean margin of Gondwana during the pre-glacial Late Ordovician. *Palaeogeogr Palaeoclimatol Palaeoecol* 294(3-4):220–231.
40. Sadler PM, Cooper RA, Melchin MJ (2011) Sequencing the graptoloid clade: Building a global diversity curve from local range charts, regional composites and global timelines. *Proc Yorks Geol Soc* 58(4):329–343.
41. Štorch P, Mitchell CE, Finney SC, Melchin MJ (2011) Uppermost Ordovician (upper Katian–Hirnantian) graptolites of north-central Nevada, U.S.A. *Bull Geosci* 86(2): 301–386.
42. Jablonski D (2002) Survival without recovery after mass extinctions. *Proc Natl Acad Sci USA* 99(12):8139–8144.
43. Holland SM, Patzkowsky ME (2015) The stratigraphy of mass extinction. *Palaeontology* 58(5):903–924.
44. Finnegan S, Heim NA, Peters SE, Fischer WW (2012) Climate change and the selective signature of the Late Ordovician mass extinction. *Proc Natl Acad Sci USA* 109(18): 6829–6834.

45. Greenacre MJ (1984) *Theory and Applications of Correspondence Analysis* (Academic, London).
46. Aikake H (1973) Information theory and an extension of the maximum likelihood principle. *Proceedings of the Second International Symposium on Information Theory*, eds Petrov BN, Caski F (Akad Kiado, Budapest), pp 267–281.
47. Boyle JT, et al. (2014) A re-examination of the contributions of biofacies and geographic range to extinction risk in Ordovician graptolites. *GFF* 136(1):38–41.
48. Finney SC, et al. (1999) Late Ordovician mass extinction: A new perspective from stratigraphic sections in central Nevada. *Geology* 27(3):215–218.
49. Ruedemann R (1947) Graptolites of North America. *Mem Geol Soc Am* 19:1–652.
50. Carter C, Churkin MJ (1977) Ordovician and Silurian graptolite succession in the Trail Creek area, Central Idaho—A graptolite zone reference section. *US Geol Surv Prof Pap* 1020:1–37.
51. Mitchell CE, Goldman D, Cone MR, Maletz J, Janousek H (2003) Ordovician graptolites of the Phi Kappa Formation at Trail Creek, Central Idaho, USA: A revised biostratigraphy. *Proceedings of the Seventh International Graptolite Conference*, eds Ortega G, Aceñolaza FG (Inst Superior Correl Geol, San Miguel de Tucumán, Argentina), pp 69–72.
52. Goldman D, et al. (2007) Ordovician graptolites and conodonts of the Phi Kappa Formation in the Trail Creek region of central Idaho: A revised, integrated biostratigraphy. *Acta Palaeontol Sin* 46(Suppl):155–162.
53. Ross RB, Berry WBN (1963) Ordovician graptolites of the Basin Ranges in California, Nevada, Utah and Idaho. *US Geol Surv Bull* 1134:1–177.
54. Melchin MJ (1987) Upper Ordovician graptolites from the Cape Phillips Formation, Canadian Arctic Islands. *Bull Geol Soc Den* 35(3-4):191–202.
55. Melchin MJ, McCracken AD, Oliff FJ (1991) The Ordovician–Silurian boundary on Cornwallis and Truro islands, Arctic Canada: Preliminary data. *Can J Earth Sci* 28(11): 1854–1862.
56. Williams SH (1982) The late Ordovician graptolite fauna of the Anceps bands at Dob's Linn, southern Scotland. *Geol Palaeontol* 16:29–56.
57. Williams SH (1983) The Ordovician–Silurian boundary graptolite fauna of Dob's Linn, southern Scotland. *Palaeontology* 26(3):605–639.
58. Melchin MJ, Holmden C, Williams SH (2003) Correlation of graptolite biozones, chitinozoan biozones, and carbon isotope curves through the Hirnantian. *Ordovician from the Andes*, eds Albanesi GL, Beresi MS, Peralta SH (Inst Superior Correl Geol, San Miguel de Tucumán, Argentina), pp 101–104.
59. Koren TN, Oradovskaya MM, Pylma LJ, Sobolevskaya RF, Chugaeva MN (1983) *The Ordovician and Silurian Boundary in the Northeast of the U.S.S.R.* (Nauka, Leningrad, Russia). Russian.
60. Koren TN, Sobolevskaja RF (2008) The regional stratotype section and point for the base of the Hirnantian Stage (the uppermost Ordovician) at Mirny Creek, Omulev Mountains, Northeast Russia. *Est J Earth Sci* 57(1):1–10.
61. Apollonov MK, Bandaletov SM, Nikitin JF (1980) The Ordovician–Silurian Boundary in Kazakhstan (Kazakh SSR, Pechat, Kazakhstan). Russian.
62. Apollonov MK, Koren TN, Nikitin IF, Paletz LM, Tsai DT (1988) Nature of the Ordovician-Silurian boundary in South Kazakhstan, U.S.S.R. *A Global Analysis of the Ordovician –Silurian Boundary*, eds Cocks LRM, Rickards RB (Nat Hist Museum, London), pp 145–154.
63. Chen X, et al. (2000) Late Ordovician to earliest Silurian graptolite and brachiopod biozonation from the Yangtze region, South China with a global correlation. *Geol Mag* 137(6):623–650.
64. Chen X, Fan JX, Melchin MJ, Mitchell CE (2005) Hirnantian (Latest Ordovician) graptolites from the Upper Yantze region, China. *Palaeontology* 48(2):235–280.
65. Chen X, et al. (2006) The global boundary stratotype section and point (GSSP) for the base of the Hirnantian Stage (the uppermost of the Ordovician System). *Episodes* 29(3):183–197.
66. Fan JX, et al. (2014) Geobiodiversity Database (GBDB) in stratigraphic, palaeontological and palaeogeographic research: Graptolites as an example. *GFF* 136(1): 70–74.
67. Brenchley PJ (2001) Late Ordovician Extinction. *Palaeobiology II*, eds Briggs DEG, Crowther PR (Blackwell, Oxford), pp 220–223.
68. Harper DA, Hammarlund EU, Rasmussen CM (2014) End Ordovician extinctions: A coincidence of causes. *Gondwana Res* 25(4):1294–1307.
69. Desrochers A, Farley C, Achab A, Asselin E, Riva JF (2010) A far-field record of the end Ordovician glaciation: The Ellis Bay Formation, Anticosti Island, Eastern Canada. *Palaeogeogr Palaeoclimatol Palaeoecol* 296(3-4):248–263.
70. Kiessling W, Martin A (2007) Environmental determinants of marine benthic biodiversity dynamics through Triassic–Jurassic time. *Paleobiology* 33(3):414–434.
71. Simpson C, Paul GH (2009) Assessing the role of abundance in marine bivalve extinction over the post-Paleozoic. *Paleobiology* 35(4):631–647.
72. Hopkins MJ, Simpson C, Kiessling W (2014) Differential niche dynamics among major marine invertebrate clades. *Ecol Lett* 17(3):314–323.
73. Foote M (2014) Environmental controls on geographic range size in marine animal genera. *Paleobiology* 40(3):440–458.
74. Connolly SR, Miller AI (2001) Joint estimation of sampling and turnover rates from fossil databases: Capture-mark-recapture methods revisited. *Paleobiology* 27(4): 751–767.
75. Foote M (2001) Inferring temporal patterns of preservation, origination, and extinction from taxonomic survivorship analysis. *Paleobiology* 27(4):602–630.
76. Metropolis N, Rosenbluth AW, Rosenbluth MN, Teller AH, Teller E (1953) Equations of state calculations by fast computing machines. *J Chem Phys* 21(6):1087–1092.
77. Hastings WK (1970) Monte Carlo sampling methods using Markov chains and their applications. *Biometrika* 57(1):97–109.
78. Wartenberg D, Ferson S, Rohlf FJ (1987) Putting things in order: A critique of detrended correspondence analysis. *Am Nat* 129(3):434–448.
79. Miller AI, Holland SM, Meyer DL, Dattilo BF (2001) The use of faunal gradient analysis for intraregional correlation and assessment of changes in sea-floor topography in the type Cincinnatian. *J Geol* 109(5):603–613.
80. Hammer Ø, Harper DAT, Ryan PD (2001) PAST: Paleontological statistics software package for education and data analysis. *Palaeontol Electronica* 4(1):4.
81. Chen Q, Fan JX, Melchin MJ, Zhang L (2014) Temporal and spatial distribution of the Wufeng Formation black shales (Upper Ordovician) in South China. *GFF* 136(1):55–59.
82. Chen X, Rong JY, Li Y, Boucot AJ (2004) Facies patterns and geography of the Yangtze region, South China, through the Ordovician and Silurian transition. *Palaeogeogr Palaeoclimatol Palaeoecol* 204(3):353–372.
83. Yan D, et al. (2015) Organic matter accumulation of Late Ordovician sediments in North Guizhou Province, China: Sulfur isotope and trace element evidences. *Mar Pet Geol* 59:348–358.
84. Shannon CE, Weaver W (1949) *The Mathematical Theory of Communication* (Univ Illinois Press, Urbana, IL).
85. Heip CHR, Herman PMJ, Soetaert K (1998) Indices of diversity and evenness. *Oceanis* 24(4):61–87.
86. Kosnik MA, Wagner PJ (2006) Effects of taxon abundance distributions on expected numbers of sampled taxa. *Evol Ecol Res* 8(2):195–211.
87. Magurran AE (2004) *Measuring Biological Diversity* (Blackwell Sci, Oxford).
88. McGill BJ, et al. (2007) Species abundance distributions: Moving beyond single prediction theories to integration within an ecological framework. *Ecol Lett* 10(10): 995–1015.
89. Mathworks (2013) *MATLAB Release 2013b* (MathWorks, Natick, MA).
90. Root RB (1967) The niche exploitation pattern of the blue-gray gnatcatcher. *Ecol Monogr* 37(4):317–350.
91. Laland KN, Odling-Smee FJ, Feldman MW (1999) Evolutionary consequences of niche construction and their implications for ecology. *Proc Natl Acad Sci USA* 96(18): 10242–10247.
92. Frontier S (1985) Diversity and structure in aquatic ecosystems. *Oceanogr Mar Biol Ann Rev* 23:253–312.
93. Gray JS (1987) *Species Abundance Patterns in Organization of Communities Past and Present*, eds Gee JHR, Gillier PS (Blackwell, Oxford), pp 53–67.
94. Cooper RA, Sadler PM, Hammer Ø, Gradstein FM (2012) The Ordovician Period. *The Geological Timescale 2012*, eds Gradstein FM, Ogg JG, Schmitz MD, Ogg GM (Elsevier, Amsterdam), Vol 1, pp 489–523.
95. Chen X, et al. (2000) Biostratigraphy of the Hirnantian Substage from the Yangtze region. *J Stratigr* 21(1):169–175.
96. Zhang L, Fan JX, Chen Q, Melchin MJ (2014) Geographic dynamics of some major graptolite taxa of the Diplograptina during the Late Ordovician mass extinction in South China. *GFF* 136(1):327–332.